

# High Slope Efficiency Measured From a Composite-Resonator Vertical-Cavity Laser

D. M. Grasso, K. D. Choquette, D. K. Serkland, G. M. Peake, and K. M. Geib

**Abstract**—We report high differential slope of the light versus current ( $L$ - $I$ ) characteristic in excess of 400% external quantum efficiency from a monolithic dual resonator vertical-cavity surface-emitting laser. The additional optical cavity of the composite resonator can provide gain or loss to the distributed laser mode, depending on the bias conditions. We describe the factors contributing to the internal optical loss, and present a qualitative model for the  $L$ - $I$  characteristic. With sufficient current injected into the top cavity, the composite-resonator vertical-cavity laser achieves over 6 W/A of differential slope efficiency from threshold to greater than 1 mW of output power, which may be applicable for analog optical data links.

**Index Terms**—Coupled cavity, optical link, slope efficiency.

## I. INTRODUCTION

VERTICAL-CAVITY surface-emitting lasers (VCSELs) offer many attractive properties for use in short-distance communications, including high modulation bandwidth, low power consumption, and relative ease of manufacturing [1]. VCSELs are being considered as a potential low-cost solution for optical-fiber-fed radio-frequency (RF) links, and data rates of over 15 Gb/s have been demonstrated with 1 km of high-bandwidth multimode fiber [2], [3]. A thorough experimental study has been conducted on the microwave properties of oxide-confined VCSELs under dc injection and direct modulation [4]. One conclusion of this prior work is that although multimode VCSELs can provide the necessary bandwidth and dynamic range to meet requirements for link gain, the differential slope efficiency of the light-current ( $L$ - $I$ ) characteristic is a significant source of RF loss in a system with direct modulation. This is in agreement with the current gain calculations for a directly modulated link given in [5]. Therefore, improvement of the slope efficiency may enable future VCSEL-based link applications. The increase in efficiency without simultaneous increase in threshold current is possible through the use of multielement devices. Previous results on cascade VCSEL arrays [6] and bipolar cascade VCSELs [7] have shown efficiencies of 180% from a  $2 \times 3$  array and 130% from a single device, respectively. Similar work using series-connected edge-emitting lasers has shown slope efficiencies of up to 390% for a 12-stage device [8].

Manuscript received November 17, 2005; revised February 6, 2006. This work was supported by National Science Foundation Grant 0121662.

D. M. Grasso and K. D. Choquette are with the Micro and Nanotechnology Laboratory, Department of Electrical and Computer Engineering, University of Illinois at Urbana-Champaign, Urbana, IL 61801 USA (e-mail: grasso@uiuc.edu).

D. K. Serkland, G. M. Peake, and K. M. Geib is with the Sandia National Laboratories, Albuquerque, NM 87185 USA.

Digital Object Identifier 10.1109/LPT.2006.873544

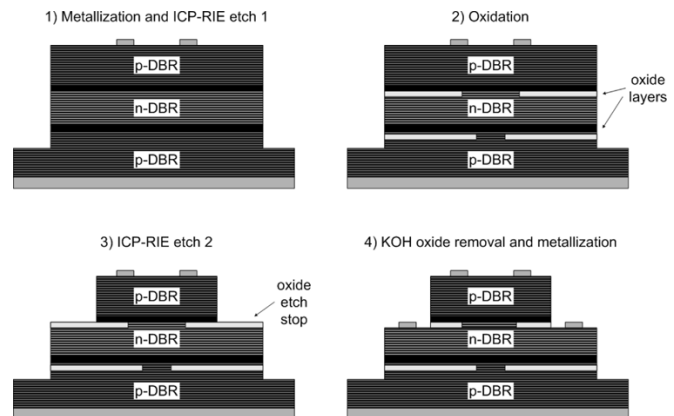


Fig. 1. CRVCL fabrication process up to planarization.

In this letter, we show high differential slope efficiency of over 6 W/A (>400% quantum efficiency at 850 nm) near threshold from a single VCSEL with two electrically independent, optically coupled active regions. This device is referred to as a composite-resonator vertical-cavity laser (CRVCL) [9], [10]. Previous work has analyzed the effect of the second optical cavity on the threshold and modal characteristics over a broad operating temperature range [11], [12]. We will discuss the fabrication of the dual oxide-confined cavity CRVCL, the continuous-wave operating characteristics, and a qualitative model of this performance.

## II. DEVICE STRUCTURE AND FABRICATION

The CRVCL in this study is grown by metal-organic chemical vapor deposition and is composed of a monolithic bottom p-type distributed Bragg reflector (DBR) with 35 periods, a middle n-DBR with 11.5 periods, and an upper p-DBR with 19 periods. Each period of the DBR consists of  $\text{Al}_{0.92}\text{Ga}_{0.08}\text{As}$ - $\text{Al}_{0.16}\text{Ga}_{0.84}\text{As}$  layers with compositional grading between them. The DBR mirrors separate two  $1\text{-}\lambda$ -thick optical cavities (where  $\lambda$  is the lasing wavelength), each of which contain five GaAs quantum wells (QWs).

The basic fabrication procedure is shown in Fig. 1. A ring contact of  $150/1500\text{-}\text{\AA}$  Ti-Au is deposited on the top surface, and a broad-area contact of  $200/2000\text{-}\text{\AA}$  Ti-Au deposited on the back side of the sample. An inductively coupled plasma reactive-ion etch (ICP-RIE) of  $\text{SiCl}_4$ -Ar is used to define an approximately  $100 \times 100\ \mu\text{m}$  lower mesa. Subsequently, a single wet oxidation of two  $\text{Al}_{0.98}\text{Ga}_{0.02}\text{As}$  layers is done to define a current aperture for each cavity. The oxide layer for the top cavity is placed in the middle n-DBR. This resulting layer is used as an etch stop for a second ICP-RIE step that defines a smaller upper

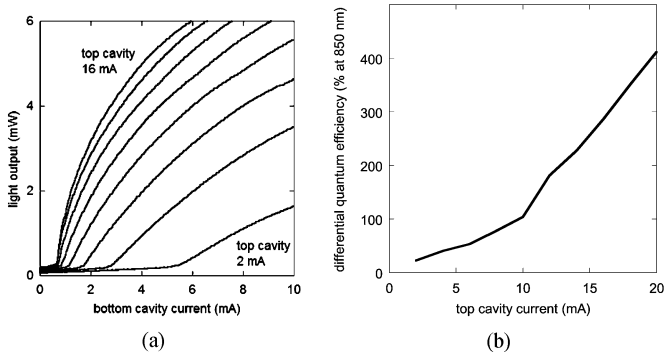


Fig. 2. (a) Light output versus bottom cavity current. Top cavity currents labeled on plot. (b) Differential quantum efficiency at threshold versus top cavity current.

mesa of approximately  $40 \times 40 \mu\text{m}$ . The oxidized layer is removed with a 45% wt KOH:H<sub>2</sub>O solution [13], and a middle ring contact of 400/200/1400-Å AuGe-Ni-Au is deposited on the layer exposed by the KOH removal. The resulting structure is shown in Fig. 1, Step 4. The CRVCL is then planarized with HD Microsystems HD-4001 polyimide to facilitate deposition of ground-signal-ground coplanar waveguide contacts for the top cavity. The CRVCL is fabricated in a double mesa structure to allow independent electrical injection into each cavity. We find that the upper oxide layer is several micrometers larger than the lower one, and thus, defines the transverse diameter of the optical cavity. We attribute the difference in oxide layer lengths to very slight epitaxial nonuniformity during material growth. The device used in this study has a lower oxide aperture of approximately  $5 \mu\text{m}$ , and an upper oxide aperture of approximately  $10 \mu\text{m}$ . Most of the CRVCLs measured cannot reach threshold with current only injected into the top cavity; this may be due to lower current confinement from the oxide aperture placement in the n-DBR as well as the larger aperture size.

### III. RESULTS AND DISCUSSION

Fig. 2(a) shows the measured  $L$ - $I$  characteristics of the CRVCL. The top cavity is held at a fixed current for each curve in Fig. 2, while the bottom cavity current is varied from 0 to 10 mA. The upper cavity current increases in steps of 2 mA between each curve. As the current in the top cavity is increased, the current in the bottom cavity required to reach threshold is reduced [11]. In addition, the differential quantum efficiency of the device increases. As shown in Fig. 2(b), if 10 mA is applied to the top cavity, the slope efficiency becomes larger than the maximum possible for a single cavity laser. Fig. 3 shows a close up of the  $L$ - $I$  characteristic corresponding to a top cavity current of 20 mA. Near threshold, the slope is approximately 6.35 W/A, which is greater than 400% differential quantum efficiency. Above threshold, the slope decreases as the bottom cavity current is increased. There are variations in the maximum slope efficiency achievable from device to device, but the results of decreasing threshold current and increased slope efficiency with increasing top cavity current are representative of all lasers tested. We have confirmed that the large slope efficiency and decrease in threshold current with increased upper cavity current persists under pulsed operation, and thus

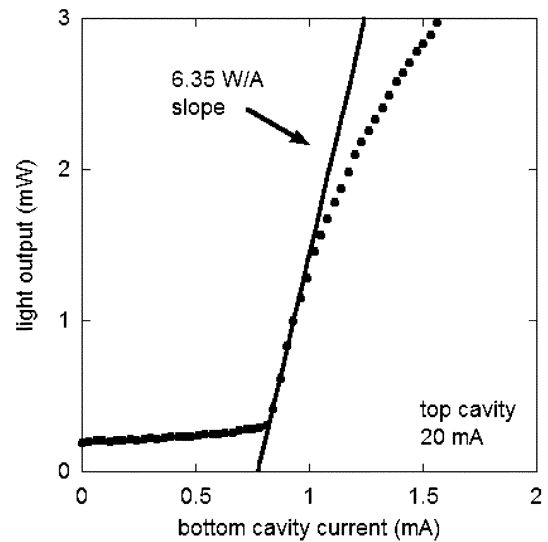


Fig. 3. Close-up of  $L$ - $I$  characteristic near threshold with top cavity current of 20 mA.

are not the result of thermal lensing effects [14]. In addition, although the CRVCL has two longitudinal resonances [8], the device in this study lases in a single longitudinal mode shifting by approximately 4 nm over the entire current range in Figs. 2 and 3. Multiple transverse modes exist at threshold, and follow a standard VCSEL modal evolution as the current in either cavity is increased [11]. Therefore, the improvement in efficiency is not related to additional modes reaching threshold as the top cavity current is increased. In the analysis that follows, we describe the gain and loss processes that contribute to the external quantum efficiency, and develop a phenomenological description that is consistent with the  $L$ - $I$  data shown in Figs. 2 and 3.

A unique feature of the CRVCL is ability to reduce the bottom cavity current required to reach threshold and simultaneously increase the slope efficiency by increasing the top cavity current. The light output  $L$  versus current injected into the bottom cavity  $I_{\text{bot}}$  above threshold is given by [15]

$$L = \eta_i \frac{\hbar\omega}{q} \frac{\alpha_m}{\alpha_i + \alpha_m} (I_{\text{bot}} - I_{\text{th}}) \quad (1)$$

where  $\eta_i$  is the internal quantum efficiency, and  $\alpha_i$  and  $\alpha_m$  are the internal and mirror losses corresponding to a threshold current of  $I_{\text{th}}$ . From (1), the key parameter changing in Fig. 2 with additional top cavity current is  $\alpha_i$ . The internal loss coefficient in a QW laser can have many contributing mechanisms. However, we can group the important processes in the CRVCL into two categories

$$\alpha_i = \alpha_0 + \alpha' (I_{\text{top}}) \quad (2)$$

where the primed term depends on the top cavity current and the  $\alpha_0$  term does not. The first term represents distributed optical loss present in every semiconductor laser. The magnitude of the primed term is determined by the material gain of the top cavity, and is negative if current is supplied to provide sufficient gain. Although the  $\alpha_i$  term in a conventional laser can also have a current dependence [16], we ignore these effects. There is an implicit temperature dependence in the  $\alpha'$  term, since an increase

in current corresponds to an increase in temperature. The current-dependent term is most important, since we are concerned with the change in efficiency with changing top cavity current. In addition, the available modal gain  $\gamma_{\text{eff}}$  in the CRVCL is determined by an effective threshold that includes the overlap of the distributed optical mode with the material gain of both active regions [17]

$$\gamma_{\text{eff}} = \Gamma_{\text{top}}g_{\text{top}} + \Gamma_{\text{bot}}g_{\text{bot}} = \alpha_0 + \alpha_m \quad (3)$$

where  $\Gamma_{\text{top}}$  and  $\Gamma_{\text{bot}}$  refer to the spatial overlap of the optical mode with the material gains  $g_{\text{top}}$  and  $g_{\text{bot}}$  of the two cavities. In addition, the spectral overlap of the two cavity resonances and material gain of each cavity can affect the threshold gain. Considering (1)–(3) together, it is evident that the additional gain or loss from the top cavity determines the slope efficiency and  $I_{\text{th}}$ .

In a conventional VCSEL, the differential slope of the  $L$ – $I$  characteristic decreases above threshold and eventually becomes negative due to spectral misalignment of the cavity resonance with the material gain of the QWs with increasing injection current. In addition, the internal quantum efficiency decreases with increasing temperature. In the CRVCL, there are two independent currents injected into the device, each of which can increase the temperature in the active regions and DBRs. Therefore, we expect the CRVCL to show the same (and possibly larger) reduction in slope efficiency with increasing current as a single-cavity VCSEL. It can be seen in Fig. 2 that as the top cavity current is increased, the change in slope efficiency is evident over a larger range of the  $L$ – $I$  characteristic. In addition, the reduction in threshold current is smaller between incremental  $L$ – $I$  curves as the top cavity current is increased and  $I_{\text{bot}}$  at maximum  $L$  decreases for  $I_{\text{top}} > 8$  mA. This phenomena is consistent with the thermal effects of a conventional VCSEL and temperature-dependent threshold current. Finally, the current-dependent mechanisms in [16] can only further increase the optical loss with increasing temperature and current.

To summarize, the increase in slope efficiency and decrease in bottom cavity current required to reach threshold is caused by the additional gain from the top cavity. This corresponds to reduction in  $\alpha_i$  near threshold as  $I_{\text{top}}$  is increased, caused by the current dependent  $\alpha'$  term in (2). The magnitude of this term is influenced by the modal gain available in (3). The corresponding increase in slope efficiency cannot be maintained over the entire  $L$ – $I$  curve, similar to a conventional VCSEL.

#### IV. CONCLUSION

We report high differential slope of the  $L$ – $I$  characteristic from a CRVCL in excess of 400% quantum efficiency from threshold to more than 1 mW of power. The increase in slope efficiency and decrease in current required to reach threshold is caused by the additional modal gain from the top cavity. Compared with previous VCSEL work in [6] and [7], the CRVCL

obtains higher efficiency, but over a smaller range of its  $L$ – $I$  characteristic. It may be possible to improve the linearity of the devices through spectral detuning of the two sets of material gains with respect to the cavity resonance or with one another, thus achieving lasing over a broader temperature range. In addition, any improvement to the internal quantum efficiency at elevated temperatures, if possible, will enhance the linearity. Further improvements of the thermal properties may enable future CRVCL applications requiring RF link gain.

#### REFERENCES

- [1] K. D. Choquette and K. M. Geib, *Vertical-Cavity Surface-Emitting Lasers*, C. Wilmsen, H. Temkin, and L. Coldren, Eds. New York: Cambridge, 1999, pp. 193–232.
- [2] P. Pepeljugoski, D. Kuchta, Y. Kwark, P. Pleunis, and G. Kuyt, “15.6 Gb/s transmission over 1 km of next generation multimode fiber,” *IEEE Photon. Technol. Lett.*, vol. 14, no. 5, pp. 717–719, May 2002.
- [3] C. Carlsson, A. Larsson, and A. Alping, “RF transmission over multimode fibers using VCSELs—comparing standard and high-bandwidth multimode fibers,” *J. Lightw. Technol.*, vol. 22, no. 7, pp. 1694–1700, Jul. 2004.
- [4] C. Carlsson, H. Matrinsson, R. Schatz, J. Halonen, and A. Larsson, “Analog modulation properties of oxide confined VCSELs at microwave frequencies,” *J. Lightw. Technol.*, vol. 20, no. 9, pp. 1740–1709, Sep. 2002.
- [5] A. S. Daryoush, E. Ackerman, N. R. Samant, S. Wanuga, and D. Kasemset, “Interfaces for high-speed fiber-optic links: Analysis and experiment,” *IEEE Trans. Microw. Theory Tech.*, vol. 39, no. 12, pp. 2031–2044, Dec. 1991.
- [6] K. D. Choquette, E. W. Young, K. M. Geib, D. K. Serkland, A. A. Allerman, C. Cox, E. Ackerman, and H. Roussel, “Cascade vertical cavity surface emitting laser arrays,” in *Proc. LEOS 2002*, vol. 1, pp. 327–327.
- [7] T. Knodl, M. Golling, A. Straub, and K. J. Ebeling, “Multi-diode cascade VCSEL with 130% differential quantum efficiency at CW room temperature operation,” *Electron. Lett.*, vol. 37, pp. 31–33, 2001.
- [8] J. T. Getty, L. A. Johansson, E. J. Skogen, and L. A. Coldren, “1.55- $\mu$ m bipolar cascade segmented ridge lasers,” *IEEE J. Sel. Topics Quantum Electron.*, vol. 9, no. 5, pp. 1138–1145, Sep./Oct. 2003.
- [9] R. P. Stanley, R. Houdre, U. Oesterle, M. Ilegems, and C. Weisbuch, “Coupled semiconductor microcavities,” *Appl. Phys. Lett.*, vol. 65, no. 16, pp. 2093–2095, 1994.
- [10] A. J. Fischer, K. D. Choquette, W. W. Chow, H. Q. Hou, and K. M. Geib, “Coupled resonator vertical cavity laser diode,” *Appl. Phys. Lett.*, vol. 75, no. 19, pp. 3020–3022, 1999.
- [11] D. M. Grasso and K. D. Choquette, “Threshold and modal characteristics of composite-resonator vertical-cavity lasers,” *IEEE J. Quantum Electron.*, vol. 39, no. 12, pp. 1526–1530, Dec. 2003.
- [12] —, “Temperature-dependent polarization characteristics of composite-resonator vertical-cavity lasers,” *IEEE J. Quantum Electron.*, vol. 41, no. 2, pp. 127–131, Feb. 2005.
- [13] R. L. Naone and L. A. Coldren, “Tapered air apertures for thermally robust VCL structures,” *IEEE Photon. Technol. Lett.*, vol. 11, no. 11, pp. 1339–1341, Nov. 1999.
- [14] N. K. Dutta, L. W. Tu, G. Hasnain, G. Zydzik, Y. H. Wang, and A. Y. Cho, “Anomalous temporal response of gain-guided surface-emitting lasers,” *Electron. Lett.*, vol. 27, no. 3, pp. 208–210, 1991.
- [15] S. L. Chuang, *Physics of Electronic Devices*. New York: Wiley, 1995.
- [16] W. Susaki, T. Oku, and T. Sogo, “Optical losses and efficiency in GaAs laser diodes,” *IEEE J. Quantum Electron.*, vol. QE-4, no. 4, pp. 122–125, Apr. 1968.
- [17] A. C. Lehman and K. D. Choquette, “Threshold gain temperature dependence of composite resonator vertical-cavity lasers,” *IEEE J. Sel. Topics Quantum Electron.*, vol. 11, no. 5, pp. 962–967, Sep./Oct. 2005.